

A Docking Study of UDP-N-Acetylglucosamine Enolpyruvyl Transferase from *Haemophilus influenzae* in Complex with Inhibitors

Hye-Jin Yoon¹, Bunzo Mikami², Hyun-Ju Park³, Jakyung Yoo³ and Se Won Suh¹

¹Department of Chemistry, College of Natural Sciences, Seoul National University, Seoul 151-747, Korea

²Laboratory of Quality Design and Exploitation, Division of Agronomy and Horticultural Science, Graduate School of Agriculture, Kyoto University, Gokasho, Uji, Kyoto 611-0011, Japan

³College of Pharmacy, Sungkyunkwan University, Suwon, Kyungki-do 440-746, Korea

Abstract

UDP-N-acetylglucosamine enolpyruvyl transferase (MurA; EC 2.5.1.7) catalyzes the first committed step of peptidoglycan biosynthesis in bacteria, i.e., transfer of enolpyruvate from phosphoenolpyruvate to UDP-N-acetyl-glucosamine. Because the crystallization condition contained a high concentration of ammonium sulfate, our inhibitor binding studies were not successful. Therefore, we employed a docking approach to investigate the inhibitor binding. Our results will be useful in structure-based design of specific inhibitors of MurA for antibacterial discovery.

1. Introduction

UDP-N-acetylglucosamine enolpyruvyl transferase (MurA; EC 2.5.1.7) catalyzes the first committed step of peptidoglycan biosynthesis in bacteria, i.e., transfer of enolpyruvate from phosphoenolpyruvate to UDP-N-acetyl-glucosamine.¹⁾ Crystal structures of MurA from *Enterobacter cloacae* (apo: PDB code 1NAW,²⁾ binary with a reaction intermediate: PDB code 1Q3G,³⁾ binary with a reaction product: PDB code 1RYW,⁴⁾ and binary with an inhibitor: PDB code 1YBG⁵⁾ and *Escherichia coli* (ternary with UDP-N-acetylglucosamine and fosfomycin: PDB code 1UAE,⁶⁾ binary with a reaction intermediate: PDB code 1A2N⁷⁾ were reported previously. We also reported crystallization of MurA from *H. influenzae*⁸⁾ and its structures were determined as a ternary complex with UDP-N-acetylglucosamine and fosfomycin (PDB code 2RL2), and as a binary complex with UDP-N-acetylglucosamine (PDB code 2RL1). Crystal structures of MurA revealed different conformations for the active site loop, which ranged from an open conformation for the ligand-free MurA from *E. cloacae* (PDB code 1NAW)²⁾ and a half-open conformation for the binary com-

plex with UDP-N-acetylglucosamine or the ternary complex with UDP-N-acetylglucosamine and fosfomycin of MurA from *H. influenzae* (PDB code 2RL2) to a closed conformation for the ternary complex of MurA from *E. coli* bound with UDP-N-acetylglucosamine and fosfomycin (PDB code 1UAE).⁶⁾

Fosfomycin is a naturally occurring broad-spectrum antibiotic and is the best-known inhibitor of MurA.⁹⁾ It is an epoxide that specifically inhibits MurA by forming a covalent adduct with a cysteine residue in the active site (Cys115 in both *E. coli* and *E. cloacae*; Cys117 in *H. influenzae*).¹⁰⁾ However, there is a high frequency of fosfomycin resistance and efforts have been made to discover new classes of MurA inhibitors.¹¹⁻¹³⁾

We tried crystallographic studies of inhibitor binding with RJW-3981 or RJW-110192¹¹⁾ but were not successful. The inhibitor RJW-110192 was not found at the expected active site of refined model, probably because a high concentration of ammonium sulfate in the crystallization medium precluded the inhibitor binding. We also tried to co-crystallize *H. influenzae* MurA in the presence of UDP-N-acetylglucosamine and the cyclic disulfide inhibitor RWJ-3981¹¹⁾ but could not obtain any crystals. Therefore,

we have employed a docking approach to investigate the inhibitor binding in the active site of *H. influenzae* MurA. Here we report the crystal structure of *H. influenzae* MurA complex with substrate UDP-N-acetylglucosamine and inhibitor RJW-110192, and the docking study of *H. influenzae* MurA with the Johnson and Johnson inhibitors: the cyclic disulfide (RWJ-3981), the pyrazolopyrimidine (RWJ-110192), and the purine analog (RWJ-140998).¹¹⁾

2. Experimentals

X-ray data collection and structure determination. Overexpression and crystallization conditions of *H. influenzae* MurA were same as described previously.⁸⁾ We could grow crystals in the presence of UDP-N-acetylglucosamine and the pyrazolopyrimidine inhibitor RWJ-110192¹¹⁾ under identical conditions. X-ray diffraction data was collected at 100 K at the BL-18B experimental station of Photon Fac-

tory, Japan. The complex structure with UDP-N-acetylglucosamine and RWJ-110192 was solved by the molecular replacement method using *H. influenzae* MurA in the presence of UDP-N-acetylglucosamine and fosfomycin (PDB code 2RL2). The model was refined with the program CNS,¹⁴⁾ including the bulk solvent correction. Several rounds of model building, simulated annealing, positional refinement, and individual B-factor refinement were then performed. Manual model building was done using the program O.¹⁵⁾ The structure figures were drawn using the program PyMOL (<http://pymol.sourceforge.net>).

Flexible docking. Flexible dockings have been performed with the Sybyl 7.0 software package¹⁶⁾ (Tripos, Inc., St. Louis, MO) based on Red-Hat Linux 7.0. The structures of fosfomycin and other inhibitors were prepared in MOL2 format using the sketcher module and Gasteiger-Huckel charges were

Table 1. Data collection and refinement statistics

A. Data collection	
Data set	UD+RWJ-110192 complex
X-ray wavelength (Å)	1.0000
Space group	<i>I</i> 222
<i>a</i> , <i>b</i> , <i>c</i> (Å)	63.8, 126.0, 126.7
Resolution range (Å)	50.0~2.15
Total/unique reflections	160,060/27,842
Completeness (%)	99.3 (95.3) ^a
R_{merge}^b (%)	8.7 (45.1) ^a
B. Model refinement	
Resolution range (Å)	30~2.30
Data completeness (%)	98.5
No. of reflections (working/free set)	19,179/2,120
R_{work}/R_{free}^c (%)	19.7/23.6
Average <i>B</i> -factors (Å ²)	
For 420 amino acid residues	32.1
For UD molecule	28.3
For 3 sulfate molecules	62.8
For 182 water molecules	34.7
R.m.s. deviations from ideal geometry	
Bond lengths (Å)/bond angles (°)	0.0060/1.20

^aValues in parentheses refer to the highest-resolution shell (2.23~2.15 Å).

^b $R_{merge} = \frac{\sum_h \sum_i |I(h)_i - \langle I(h) \rangle|}{\sum_h \sum_i I(h)_i}$, where $I(h)$ is the intensity of reflection h , \sum_h is the sum over all reflections, and \sum_i is the sum over i measurements of reflection h .

^c $R = \frac{\sum |F_{obs}| - |F_{calc}|}{\sum |F_{obs}|}$, where R_{free} is calculated for a randomly chosen 10% of reflections, which were not used for structure refinement and R_{work} is calculated for the remaining reflections.

assigned to the ligand atoms. The minimization was run until converged to a maximum derivative of $0.001 \text{ kcal mol}^{-1} \text{ \AA}^{-1}$, and the final coordinates were stored in a database. The crystal structure of *H. influenzae* MurA complexed with the substrate UDP-N-acetylglucosamine and fosfomycin (PDB code 2RL2) was used as a target for flexible docking. All crystallographic water molecules were removed and the active site was defined as all the amino acid residues enclosed within a sphere of 8 \AA radius centered around the bound fosfomycin. UDP-N-acetylglucosamine was also included in the active site as a heteroatoms file after fixing the atom types. The main settings were set with 1,000 solutions in order to generate the maximum conformers per each compound during FlexX docking. The 'assign formal charge, if necessary' and 'place particle' options were turned on. The scores for all FlexX solutions were calculated by the consensus scoring function (Cscore)¹⁶ and used for database ranking. One of

the conformers having the highest consensus score (Cscore = 5) was selected by visual inspection and was docked into *H. influenzae* MurA, resulting in the docking models shown in Fig. 2.

3. Results and Discussion

The complex crystal with substrate UDP-N-acetylglucosamine and inhibitor RWJ-110192 could improve with the reservoir solution of 1.8 M ammonium sulfate and 5~10% (v/v) glycerol by co-crystallization. X-ray diffraction data of the complex crystal was collected at 100 K at the BL-18B experimental station of Photon Factory, Japan, under further-optimized cryo conditions (25% glycerol and 1.8 M ammonium sulfate). The crystal has unit cell parameters of $a = 63.8 \text{ \AA}$, $b = 126.0 \text{ \AA}$, $c = 126.7 \text{ \AA}$ in the $I222$ (or $I2_12_12_1$) space group. We have refined model to reasonable R values with excellent stereochemistry at 2.3 \AA (Table 1). The model accounts

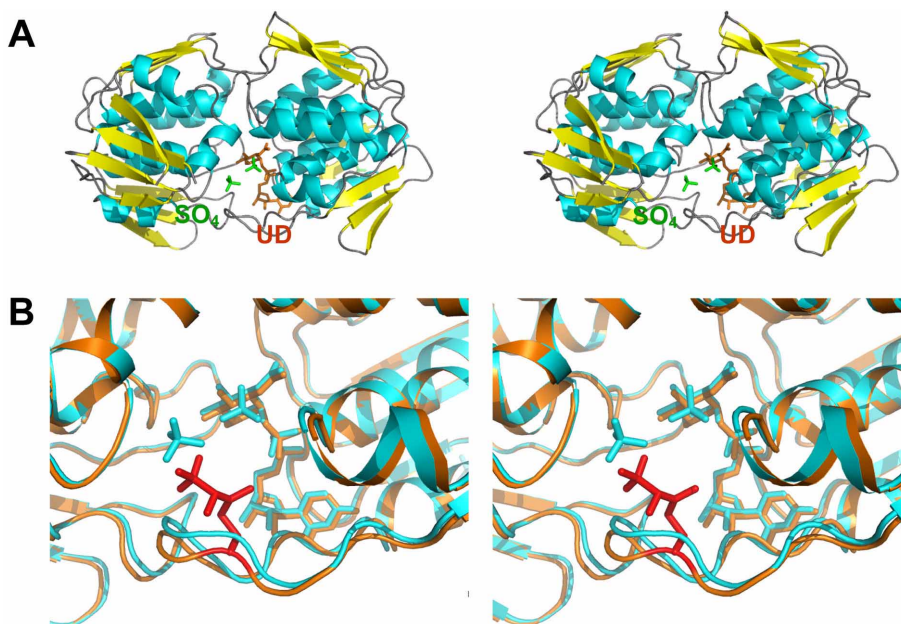


Fig. 1. (A) Stereo ribbon diagram. UDP-N-acetylglucosamine (UD, orange) and sulfates (SO_4 , green) are shown in a ball-and-stick model. α -Helices, β -strands, and loops are colored in cyan, yellow, and grey, respectively. (B) Stereo view of superimposed structures with substrate and inhibitor of *H. influenzae* MurA at active site. Ribbon models for *H. influenzae* MurA with UDP-N-acetylglucosamine and R JW-110191 (could not see binding model), and *H. influenzae* MurA with UDP-N-acetylglucosamine and fosfomycin (PDB code 2RL2) are colored in cyan and orange, respectively. Two UDP-N-acetylglucosamine, fosfomycin bound Cys117 (red), and sulfate ions are shown in a ball-and-stick model.

for 420 residues (residues 1-420), UDP-N-acetylglucosamine, three sulfate ions, and 182 water molecules (Fig. 1A). In structure, electron density is missing for C-terminal three residues (421-424) of MurA as well as all eight residues belonging to the

C-terminal fusion tag (LEHHHHHH), presumably because they are disordered in the crystal. However, the refined structure did not reveal the inhibitor bound at the active site, probably because a high concentration of ammonium sulfate in the crystalli-

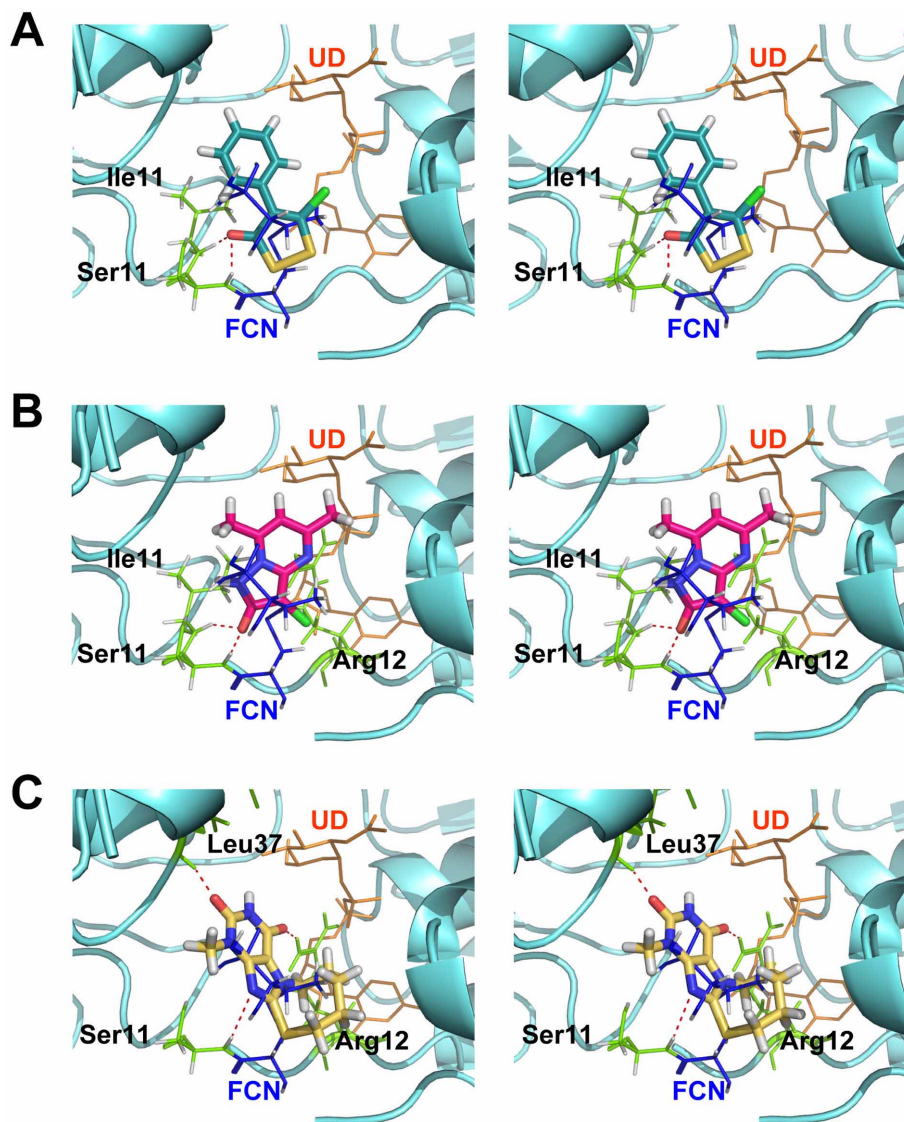


Fig. 2. Stereo view of docked poses of RJW3981 (A), RJW110192 (B), and RJW140998 (C) in the fosfomycin-binding site of *H. influenzae* MurA. The amino acid residues involved in hydrogen bonds within the binding site are represented by stick models in the ribbon diagram of *H. influenzae* MurA. The X-ray pose of fosfomycin (navy-blue) covalently attached to Cys117 and UDP-N-acetylglucosamine (orange) are also shown in a ball and stick model (PDB code 2RL2). The bound inhibitors are rendered in capped stick and their carbon atoms are colored in cyan (RJW-3981), magenta (RJW-110192), and yellow (RJW-140998), respectively. Hydrogen bonds with shorter than 3.0 Å distances are indicated by red dotted lines.

zation medium precluded the inhibitor binding (Fig. 1A). We also tried to co-crystallize *H. influenzae* MurA in the presence of UDP-N-acetylglucosamine and the cyclic disulfide inhibitor RWJ-3981¹¹⁾ but could not obtain any crystals.

Because the refined model has just a substrate UDP-N-acetylglucosamine as binary complex, we compared the structure with the UDP-N-acetylglucosamine and fosfomycin complex as ternary complex (PDB code 2RL2). The UDP-N-acetylglucosamine complex structure of *H. influenzae* MurA is highly similar to its UDP-N-acetylglucosamine and fosfomycin complex, with a root-mean-square (r.m.s.) deviation of 0.32 Å for 420 Ca atom pairs, with a maximum Ca deviation of 1.6 Å for Ser 118 (Fig. 1B). These results indicate that, in *H. influenzae* MurA, no large movement of the active site loop occurs upon binding inhibitor and the UDP-N-acetylglucosamine complex structure (although RWJ-110192 was not bound in the structure) remains in the half-open conformation as the UDP-N-acetylglucosamine and fosfomycin complex.

Since we could not experimentally observe the binding of MurA inhibitors (RJW-3981, and RJW-110192),¹¹⁾ have performed docking studies to examine their possible binding modes. The docked conformer of each inhibitor with the highest consensus binding score from FlexX is shown in Fig. 2. The inhibitors are positioned at the fosfomycin-binding site of *H. influenzae* MurA, contacting the catalytic Cys117 and forming hydrogen bonds with neighboring amino acid residues (Ser118 and/or Ile119). 1,2-Dithiole-3-one ring (a Michael acceptor) of RJW-3981 is in close contact with the sulfur of Cys117, suggesting that the Michael addition reaction possibly occurs, and the carbonyl oxygen atom forms a strong bidentate hydrogen bond with backbone NH atoms of Ser118 and Ile119 (Fig. 2A). The pyrazolopyrimidine ring of RJW-110192 also forms hydrogen bonds with the backbone NH atoms of Ser118 and Ile119, and the guanidino group of Arg122 (Fig. 2B). Docked RJW-140998 is superimposed over the X-ray pose of fosfomycin with the hydrogen bond network centered on the xanthine ring moiety (Fig. 2C). A nitrogen atom of the imidazole moiety forms a hydrogen bond with

Ser118, and one of the carbonyl oxygens of the pyrimidindione ring is involved in a hydrogen bond with the guanidino group of the conserved Arg122. In addition, the other carbonyl oxygen of pyrimidindione forms a hydrogen bond with the backbone NH atom of Leu372 in the loop located far away from the loop containing residues Cys117-Ile119. The tight interaction of bulky RJW-140998 with amino acid residues surrounding the fosfomycin-binding site may block the entrance of the second substrate phosphoenolpyruvate to UDP-N-acetylglucosamine bound in the active site (Fig. 2C). In summary, we employed a docking approach to investigate the MurA inhibitor binding. Our results will be useful in structure-based design of specific inhibitors of MurA for antibacterial discovery.

Acknowledgements

We thank Dr. E. Z. Baum at Johnson & Johnson Pharmaceutical Research and Development for providing the MurA inhibitors (RWJ-3981 and RWJ-110192). We thank beamline staffs for assistance during data collection at Photon Factory (BL-18B). This work was supported by the Basic Research Promotion Grant of Korea Research Foundation, Ministry of Education and Human Resources Development of the Korean government to HJY (KRF-2005-075-C00018).

References

- 1) Bugg, T. D. and Walsh, C. T., *Nat. Prod. Rep.*, **9**, 199 (1992).
- 2) Schonbrunn, E., Sack, S., Eschenburg, S., Perrakis, A., Krekel, F., Amrhein, N. and Mandelkow, E., *Structure*, **4**, 1065 (1996).
- 3) Eschenburg, S., Kabsch, W., Healy, M. L. and Schonbrunn, E., *Journal of Biological Chemistry*, **278**, 49215 (2003).
- 4) Eschenburg, S., Priestman, M. and Schonbrunn, E., *Journal of Biological Chemistry*, **280**, 3757 (2005).
- 5) Eschenburg, S. and Schonbrunn, E., *Proteins-Structure Function and Genetics*, **40**, 290 (2000).
- 6) Skarzynski, T., Mistry, A., Wonacott, A., Hutchinson, S. E., Kelly, V. A. and Duncan, K.,

- Structure*, **4**, 1465 (1996).
- 7) Skarzynski, T., Kim, D. H., Lees, W. J., Walsh, C. T. and Duncan, K., *Biochemistry*, **37**, 2572 (1998).
 - 8) Yoon, H. J., Ku, M. J., Ahn, H. J., Lee, B. I., Mikami, B. and Suh, S. W., *Molecules and Cells*, **19**, 398 (2005).
 - 9) El Zoeiby, A., Sanschagrín, F. and Levesque, R. C., *Mol. Microbiol.*, **47**, 1 (2003).
 - 10) Kahan, F. M., Kahan, J. S., Cassidy, P. J. and Kropp, H., *Ann. N. Y. Acad. Sci.*, **235**, 364 (1974).
 - 11) Baum, E. Z., Montenegro, D. A., Licata, L., Turchi, I., Webb, G. C., Foleno, B. D. and Bush, K., *Antimicrobial Agents and Chemotherapy*, **45**, 3182 (2001).
 - 12) DeVito, J. A., Mills, J. A., Liu, V. G., Agarwal, A., Sizemore, C. F., Yao, Z., Stoughton, D. M., Cappiello, M. G., Barbosa, M. D., Foster, L. A. and Pompliano, D. L., *Nat. Biotechnol.*, **20**, 478 (2002).
 - 13) Molina-Lopez, J., Sanschagrín, F. and Levesque, R. C., *Peptides*, **27**, 3115 (2006).
 - 14) Brunger, A. T., Adams, P. D., Clore, G. M., DeLano, W. L., Gros, P., Grosse-Kunstleve, R. W., Jiang, J. S., Kuszewski, J., Nilges, M., Pannu, N. S., Read, R. J., Rice, L. M., Simonson, T. and Warren, G. L., *Acta Crystallographica Section D-Biological Crystallography*, **54**, 905 (1998).
 - 15) Jones, T. A., Zou, J. Y., Cowan, S. W. and Kjeldgaard, M., *Acta Crystallog. Sect. A*, **47**, 110 (1991).
 - 16) Sybyl. 6.8 ed.; SYBYL molecular modeling software. Tripos Inc, St. Louis, MO (2000).